International Immunology, Vol. 10, No. 9, pp. 1289–1298

Functional expression of the MHC class I-related receptor, FcRn, in endothelial cells of mice

Jozef Borvak[1,4], James Richardson[2], Cornel Medesan[1,5], Felicia Antohe[3], Caius Radu[1], Maya Simionescu[3], Victor Ghetie[1] and **E. Sally Ward[1]**

[1]Department of Microbiology and Cancer Immunobiology Center, University of Texas Southwestern Medical Center, Dallas, TX 75235-8576, USA
[2]Department of Pathology, University of Texas Southwestern Medical Center, Dallas, TX 75235, USA
[3]Institute of Cellular Biology and Pathology 'Nicolae Simionescu', Str. Hasdeu 8, 79691 Bucharest, Romania

[4]Present address: Institute of Virology, Slovak Academy of Sciences, Dubravska cesta 9, 84246 Bratislava, Slovak Republic
[5]Present address: Institute of Virology, Center of Immunology, Sos. Mihai Bravu 285, 79650 Bucharest, Romania

Keywords: endothelial cell, FcRn, IgG

Abstract

Our recent data indicate that the MHC class I-related receptor, FcRn, plays a role in regulating serum IgG levels, in addition to its known role in transferring IgG from mother to young. In the current study, the distribution of FcRn in adult mice has been investigated using several approaches. First, tissue distribution of anti-FcRn F(ab′)$_2$, murine IgG1 and recombinant, IgG1-derived Fc-hinge fragments has been analyzed, and these FcRn binding proteins localize predominantly in skin and muscle with lesser amounts in liver and adipose tissue. Second, histochemical analyses of muscle and liver with anti-FcRn F(ab′)$_2$ indicate that FcRn is expressed in the endothelium of small arterioles and capillaries, but not in larger vessels such as the central vein and portal vasculature. Third, immunoprecipitation and immunofluorescence studies of cultured murine endothelial cells show that functional FcRn is expressed in these cells, and is located within vesicular structures in the cytosol and not on the membrane. Taken together the data demonstrate that FcRn is expressed in functionally active form in endothelial cells, indicating that these cells are a possible site at which serum IgG homeostasis is maintained.

Introduction

Recent studies in β_2-microglobulin (β_2m)-deficient mice have indicated that the MHC class I-related receptor, FcRn, plays a role in regulating serum IgG levels (1–3) in addition to mediating the transfer of maternal IgG to young rodents (4). Consistent with this, the region of mouse IgG1 that controls serum persistence closely overlaps with that involved in mediating transcytosis and binding to recombinant, soluble FcRn (5,6) and a recombinant, randomly mutated Fc fragment that binds with higher affinity to FcRn has a longer serum persistence (7). In further support of a more diverse role for FcRn than was originally postulated, FcRn α chain mRNA has been found not only in tissues involved in maternofetal transfer of IgG (brush border, yolk sac and placenta) but also in other tissues of adult animals (1,8–10) including endothelial cells (1). In addition, FcRn has been detected at the protein level in parenchymal cells of liver (10) and, in a review paper, reported to be present in endothelial cells of human muscle vasculature (11). This suggests that these cells may be involved in maintaining IgG homeostasis by recycling IgG back into the circulation following fluid-phase endocytic uptake and binding to FcRn in slightly acidic endosomal compartments, as originally hypothesized in less specific detail by Brambell (12). In this model, IgG homeostasis is maintained due to the saturable nature of FcRn, with excess IgGs being destined for degradation due to their lack of interaction with this Fc receptor. Paradoxically, the cells in

Correspondence to: E. S. Ward

Transmitting editor: A. McMichael

Received 9 February 1998, *accepted* 14 March 1998

which IgGs are broken down are also the site of IgG salvage and recycling into the serum.

The selective distribution of injected radioactive IgG into skin, muscle and liver of rats (13), mice (14) and monkeys (15) led to the suggestion that IgG catabolism is a diffuse process occurring primarily in these tissues. These results are consistent with the hypothesis that endothelial cells present in these and other organs are the sites of IgG breakdown (16,17). To date, however, the cell types involved in IgG breakdown and recycling have not been identified.

In this study, the cellular sites of FcRn expression have been analyzed by studying the tissue distribution in mice of a radiolabeled anti-FcRn $F(ab')_2$ fragment and recombinant Fc-hinge fragments that differ in their binding affinity for FcRn. Comparative tissue localization analyses of murine IgG1 (mIgG1) have also been carried out in wild-type and β_2m-deficient mice that do not express functional FcRn. In addition, FcRn expression in muscle, liver and cultured endothelial cells has been investigated by immunohistochemistry, immunofluorescence and/or immuno-precipitation analyses. Taken together, the results indicate that the endothelial cells in skin, muscle and liver are the primary sites of functional FcRn expression in adult mice and, by extension, these cells may be the major sites of serum IgG homeostasis.

Methods

Cell lines

The mouse SV40-transformed endothelial cell line derived from lymph nodes of C3H/HeJ mice (SVEC) (18) and, as negative control, the mouse T cell hybridoma 2B4 (19) were used. RMA cells are a mutagenized non-selected subclone of RBL-5, a Rauscher virus-induced murine T cell lymphoma of C57BL/6 origin (H-2^b) (20), and were used to absorb anti-β_2m and anti-MHC class I cross-reactivities of the anti-FcRn antibody made by immunizing rabbits with recombinant FcRn (see below).

Preparation of recombinant Fc-hinge fragments

Recombinant wild-type Fc-hinge fragment and the mutated Fc-hinge fragment H310A/Q311N-H433A/N434Q were expressed in *Escherichia coli* and purified using Ni^{2+}-NTA agarose as described previously (21). In binding studies using surface plasmon resonance, wild-type Fc-hinge bound to immobilized FcRn with an affinity in the nanomolar range, whilst the mutant had an affinity at least 1000 times lower (6).

Preparation of anti-FcRn antibodies

Two New Zealand rabbits were hyperimmunized with 100 μg recombinant mouse FcRn (6) emulsified in complete/incomplete Freund's adjuvant by s.c. injection at intervals of 2 weeks until suitable titers had been reached. Total rabbit IgG was isolated from sera obtained before immunization (preimmune 'control' IgG) and at the end of the hyperimmunization period (anti-FcRn IgG) by affinity chromatography on Protein A–Sepharose (Pharmacia, Piscataway, NJ). The IgGs were digested with insoluble pepsin (Sigma, St. Louis, MO) at pH 4.0 in 0.1 M acetate buffer for 4 h at which time all IgG was completely hydrolysed. Purified $F(ab')_2$ fragments were obtained by affinity chromatography on Protein A–Sepharose to remove traces of undigested IgG followed by ultracentrifugation on 30 kDa cut-off filters (Amicon, Beverly, MA) to remove low mol. wt polypeptides resulting from the pepsin digestion. The anti-FcRn $F(ab')_2$ preparation was further purified by affinity chromatography on FcRn–Sepharose (1.5 mg recombinant FcRn bound to 1 ml CNBr-activated Sepharose CL-4B). The bound fractions were eluted and radioiodinated, and then absorbed with mouse RMA cells (20) (positive for MHC class I antigen, negative for FcRn) to remove 10% of cross-reacting anti-β_2m/MHC class I antibody (300 μg $[^{125}I]F(ab')_2$ anti-FcRn incubated successively 3 times with 10^7 cells). The final preparation was centrifuged for 30 min at 14,000 *g* to remove cell debris. It did not bind at detectable levels (analyzed by flow cytometry) to MHC class I-bearing RMA cells and was completely absorbed by FcRn–Sepharose. This antibody was used for catabolism, distribution experiments and localization of FcRn in SVEC cells.

A second anti-FcRn antibody was made more recently by immunizing two rabbits with a FcRn-derived peptide (YCLNGEEFMKFNPRIG) coupled to BSA through a thioether bond. This peptide is derived from the α2 domain of mouse FcRn and the human homologue was used previously (22) to generate anti-human FcRn antibodies. The antibody bound to recombinant FcRn (6) in ELISA. The $F(ab')_2$ fragment of the anti-FcRn peptide antibody was obtained as described above. This antibody was used for the detection of FcRn in the endothelial cells of muscle and liver and in SVEC cells.

Radiolabeling of proteins

Mouse IgG1, $F(ab')_2$ fragments and recombinant Fc-hinge fragments (wild-type and mutant) were radioiodinated using $Na^{125}I$ (Amersham, Rockville, MD) and Iodo-Gen-coated tubes as previously described (21).

Catabolism and tissue distribution

Swiss mice (25–35 g) (Taconic, Germantown, NY) were fed with 0.01% NaI in drinking water 1 day prior to injection and throughout the entire period of the experiment. The animals were injected into the tail vein with $5–8\times10^7$ c.p.m./5–10 μg of protein and bled retro-orbitally after 3 min to measure the total radioactivity/amount injected. After 3 days the animals were again bled retro-orbitally, anesthetized with Metofane (Pitman-Moore, Mundelein, IL) and perfused through the heart with 50 mM HEPES-buffered saline (pH 7.2–7.4) at room temperature. When the perfusion was complete (liver completely discolored) various tissues were removed either completely (liver, kidneys, lungs, spleen, stomach, small intestine, large intestine and heart) or in weighed aliquots (skin, muscle and fat) and the radioactivity per weighed organ or aliquot measured. Total tissue weights for muscle, skin and fat were calculated as percent of the body weight based on previous measurements on three non-treated mice as recommended by Caster *et al.* (23). The extent of protein degradation was estimated by determining the amount of TCA (10%) soluble radioactivity as recommended by Strobel *et al.* (24). The half-lives of radiolabeled $F(ab')_2$ preparations and wild-type Fc-hinge were determined as previously described for Fc-hinge fragments (21).

β_2m-deficient mice (C57BL/6 background, Jackson

Laboratories, Bar Harbor, ME) and C57BL/6 controls (Jackson Laboratories) were injected with radioiodinated mouse IgG1 ($3–5\times10^6$ c.p.m./μg) and the organ distribution analyzed as above.

Localization of FcRn on SVEC cells by immunofluorescence

SVEC cells were cultured in DMEM supplemented with 15% FCS. Forty eight hours prior to staining the cells were seeded at 1×10^5 cells/ml on 12 mm diameter glass coverslips (Sigma). The attached cells were washed with DMEM (at 37°C) and fixed with cold methanol (–20°C) for 5 min at 4°C. To block the non-specific binding, the cells were treated with 2% BSA in 57 mM borate buffer (BSA-BB) pH 8.2 (for 30 min) as described by Roberts *et al.* (25). Cells were then incubated with rabbit anti-FcRn $F(ab')_2$ (250 μg/ml; preabsorbed on RMA cells) or rabbit anti-FcRn peptide $F(ab')_2$ in 1:2 diluted BSA-BB in a humidified chamber for 1 h at 37°C. After brief washing in BSA-BB, cells were exposed for 1 h to biotinylated donkey anti-rabbit $F(ab')_2$ fragment (Amersham, Arlington Heights, IL) at a 1:75 dilution. The cells were washed again (as above) and stained with streptavidin–Texas Red (Amersham; 1:50 dilution) for 1 h. The coverslips were thoroughly washed, mounted in Slow-fade (Molecular Probes, Eugene, OR), and examined with a Microphot SA Nikon microscope equipped with a Hg 100 W lamp for epifluorescence and filter combinations for Texas Red (G-1B). Images were photographed with a Microflex UFX-DX device on a T-MAX 400 ASA Kodak film.

In other experiments, the methanol-permeabilized cells were incubated with wild-type Fc-hinge (1 μg/ml) in PIPES buffer, pH 6.3, for 1 h at 37°C. After fixation of the receptor–ligand complex with 2% formaldehyde in PBS and quenching with 50 mM NH_4Cl in PBS, the cells were further exposed to anti-FcRn $F(ab')_2$ and immunolabeled under the same conditions as described above. As a further control for specificity, experiments were carried out in the absence of anti-FcRn antibody.

Affinity chromatography and immunoprecipitation

SVEC cells ($1–5\times10^7$) were suspended in 5 ml of PBS, pH 7.5, then 2.5 ml sulfo-NHS-biotin in PBS (1 mg/ml) was added. The mixture was incubated at room temperature with rotation for 30 min. After washing with PBS the pellet was resuspended in 5 ml of lysis buffer (LB), pH 8, as recommended by Blumberg *et al.* (10) but using CHAPS (Pierce, Rockford, IL) (0.5%) instead of Nonidet P-40 (1%). Following 30 min incubation on ice the suspension was centrifuged at 14,000 *g* for 5 min followed by ultracentrifugation at 50,000 *g* for 30 min. The supernatant was diluted 5-fold with LB without CHAPS and the pH adjusted to 6.0. The diluted supernatant was loaded onto a murine IgG1–Sepharose column (1.0×2.4 cm) equilibrated at pH 6.0 with PBS containing 0.1% CHAPS and the other components of LB. Following extensive washings with at least 10 column volumes at pH 6.0, the bound protein was eluted with the equilibration buffer, pH 7.5. Bound and eluted fractions were collected and concentrated by ultrafiltration. Aliquots of the pH 6.0 and 7.5 column washes were analyzed by SDS–PAGE followed by Western blotting with streptavidin–horseradish peroxidase (HRP; ICN, Costa Mesa, CA) to assess the specificity of the IgG–Sepharose. The remainders of the concentrated samples (~0.5 ml) were precleared by addition of 20 μl preimmune rabbit serum and 20 μl 12.5% (w/v) suspension of Protein A–Sepharose. Precleared supernatants (250 μl) were then incubated with Protein A–Sepharose (20 μl) in the presence of 20 μl of rabbit anti-mouse FcRn polyclonal antibody. The mixtures were incubated at 4°C overnight or at room temperature for 2–4 h. After centrifugation and extensive washings the pellets were analyzed by SDS–PAGE followed by Western blotting with streptavidin–HRP (26). Bound streptavidin–HRP conjugate was detected using enhanced chemiluminescence (Amersham).

Tissue autoradiography

SWISS mice were injected i.v. with ^{125}I-labeled proteins (~$5–8\times10^7$ c.p.m./50 μg). At 8 and 24 h post-injection the animals were anesthetized, perfused, and the muscle and skin harvested. The tissues were fixed in 2% glutaraldehyde for 12–16 h at 4°C. After fixation the tissues were washed through with several changes of 70% ethanol. The tissue was then dehydrated through graded ethanols, cleared in xylene and infused with paraffin. Sections (5 μm) were floated onto Vectabond-treated slides (Vector, Burlingame, CA). The slides were dried at 60°C for 1 h, dewaxed in xylene and the residual xylene was removed with changes of 100% ethanol. The slides were air dried, dipped in K.5 nuclear emulsion (Polysciences, Warrington, PA) and exposed for 21 days at 4°C. The slides were then developed in D19 (Kodak, Rochester, NY), counterstained with hematoxylin, and examined using brightfield and dark-field microscopy. Immunohistochemistry for Von Willebrand's Factor VIII antigen was performed on sections contiguous to those used for autoradiography. Following deparaffinization and hydration of the sections, antigen was unmasked with 0.1% pronase E/PBS for 30 min at room temperature. Non-specific secondary binding was blocked with 2% normal goat serum/PBS and 5% BSA. The primary antibody (Sigma) was diluted 1:8000 in 2% normal goat serum/5% BSA and incubated at 4°C overnight. Following washes in PBS, biotinylated goat anti-rabbit antibody diluted at 1:200 was applied to the sections. Endogenous peroxidase was quenched in 0.3% H_2O_2/CH_3OH for 30 min. Following a series of washes in PBS, streptavidin–HRP diluted at 1:500 in PBS was applied to the slides and incubated for 30 min. Following PBS washes, the chromogen, 3.3′-diaminobenzidine (DAB Dako, Carpinteria, CA) was added. The slides were washed, counterstained with hematoxylin, rinsed in water, dehydrated through graded ethanol and coverslipped with Permount. Substitution of the primary antibody with PBS served as a control for non-specific binding.

Immunohistochemistry

Muscle and liver from SCID mice (Taconic) were harvested and fixed in 10% buffered formalin overnight, dehydrated through graded ethanol, and embedded in paraffin. Sections were cut at 5 μm onto Vectabond-treated slides and air dried. Following deparaffinization and dehydration, sections were microwaved in citrate buffer pH 7.0 at 1350 watts for 5 min followed by an additional 5 min at 900 watts. Non-specific binding was blocked by incubating the sections for 30 min in 2% normal goat serum and 5% BSA. The sections were incubated overnight in a humid chamber with rabbit $F(ab')_2$

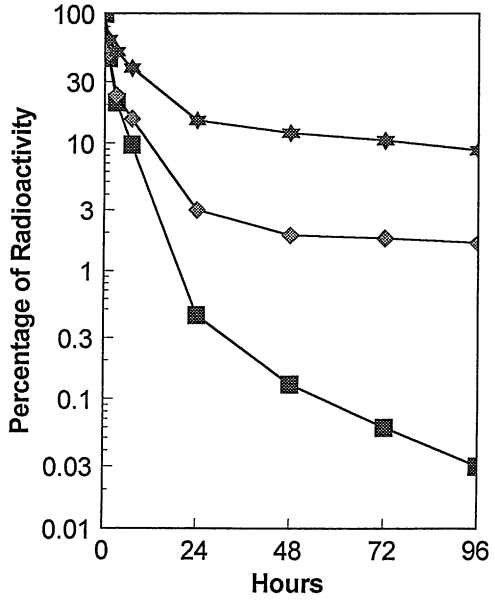

Fig. 1. Clearance curves of rabbit anti-FcRn F(ab′)$_2$, preimmune rabbit F(ab′)$_2$ and wild-type Fc-hinge fragments in Swiss mice. The β phase half-lives are: anti-FcRn F(ab′)$_2$, 78.2 ± 4.8 h (four animals) (◆); preimmune F(ab′)$_2$, 24.6 ± 3.6 h (three animals) (■); wild-type Fc-hinge, 84.3 ± 18.0 (three animals) (★).

anti-FcRn peptide antibody at a dilution of 1:600–1:1,200. Following washes in PBS, biotinylated goat anti-rabbit F(ab′)$_2$ diluted at 1:200 (Vector) was added to the sections for 30 min. Endogenous peroxidase was quenched in 0.3% H_2O_2/CH_3OH for 30 min. Streptavidin–HRP at 2 μg/ml (Vector) was applied and incubated for 30 min, rinsed with PBS and developed with DAB (Dako). Sections were counterstained with hematoxylin, rinsed in water, dehydrated through ethanols and cover-slipped with Permount. Substitution of the primary antibody with PBS served as control for non-specific binding.

Results

Clearance of F(ab′)$_2$ fragments from the circulation

To avoid cross-reactivity with β_2m/MHC class I, anti-FcRn F(ab′)$_2$ fragment made by immunizing rabbits with soluble recombinant FcRn (6) was preabsorbed with MHC class I-expressing RMA cells prior to use. The elimination curves for radiolabeled rabbit anti-FcRn F(ab′)$_2$, preimmune rabbit F(ab′)$_2$ and wild-type Fc-hinge fragments are shown in Fig. 1. Over 90% of the radioactivity in the serum samples from each time point was TCA precipitable. HPLC analyses showed that the mol. wt of the radiolabeled F(ab′)$_2$ fragments in the serum at 24 h were identical to those of the injected proteins (data not shown), indicating that the F(ab′)$_2$ fragments were not associating with other serum proteins. The α phase, which is the initial phase (approximately the first 24 hours post-injection) of clearance and represents equilibration of the injected proteins between the intra- and extravascular space, was similar for both preimmune and anti-FcRn F(ab′)$_2$. In contrast, the β phase half-life of the anti-FcRn F(ab′)$_2$, which represents the clearance of the equilibrated molecules from the intravascular space, is significantly longer than that of the preimmune F(ab′)$_2$ (78 versus 25 h) and is close to that of the wild-type Fc-hinge fragment. A possible explanation for this behavior is that the anti-FcRn F(ab′)$_2$ molecules bind to FcRn in the cells involved in regulating serum IgG levels and, similarly to IgG, a fraction is recycled into the circulation by a transcytotic-like process (27).

Tissue distribution of F(ab′)$_2$ fragments

The recovery of the injected radioactivity (expressed as percentage of injected dose) in tissues following administration of the F(ab′)$_2$ fragments was determined at an interval of time (3 days) when >98% of the injected radioactivity had been lost from the circulation. The intravascular radioactivity of the tissues was rendered negligible by perfusion that resulted in almost total recovery of serum radioactivity levels in the perfusate (data not shown).

From Fig. 2 it can be seen that there are two major sites (skin and muscle) where both anti-FcRn F(ab′)$_2$ and the preimmune F(ab′)$_2$ fragments are preferentially localized. The quantitative differences in the distribution expressed as either percentage of injected dose or specific distribution (c.p.m./μg tissue) clearly show that the anti-FcRn F(ab′)$_2$ fragment preferentially distributes in skin and muscle, and to a much lesser extent in adipose tissue and liver (Fig. 2). The ratio between the distribution of anti-FcRn F(ab′)$_2$ and preimmune F(ab′)$_2$ fragments is 4.2 for skin, 3.7 for adipose tissue, 3.0 for muscle and 2.4 for liver, and with the exception of liver these differences are highly significant (by two-paired Student *t*-test; $P = 0.0069$ for fat, $P = 0.036$ for muscle, $P = 0.0278$ for skin and $P = 0.1137$ for liver). Comparison of the localization of the two F(ab′)$_2$ preparations in these tissues clearly confirms that skin and muscle, and to a lesser extent adipose tissue and liver, selectively accumulate anti-FcRn F(ab′)$_2$ fragment. In contrast, the preimmune F(ab′)$_2$ fragment preferentially accumulates in the kidneys relative to the anti-FcRn F(ab′)$_2$, probably as a result of the inability of this F(ab′)$_2$ fragment to be retained by FcRn binding in the tissues involved in IgG homeostasis. As a result, this F(ab′)$_2$ fragment is available for renal elimination to a greater extent than the anti-FcRn F(ab′)$_2$ fragment. TCA extraction of the various tissues showed that the majority of the radioactivity was TCA insoluble from mice injected with either anti-FcRn F(ab′)$_2$ (76.6–97.7%) or preimmune F(ab′)$_2$ (62.6–93.1%) fragment and the differences between tissues were not statistically significant. For this reason, percentages of injected doses are calculated using total c.p.m., rather than TCA-precipitable c.p.m. for the data shown in Fig. 2.

Autoradiography of the muscle tissue at 8 and 24 h after injection of either anti-FcRn F(ab′)$_2$ or preimmune F(ab′)$_2$ fragment showed a significant concentration of silver grains only for the anti-FcRn F(ab′)$_2$ antibody at 8 h post-injection. The lumens of small arterioles and venules were, with a few exceptions, free of silver grains indicating that the perfusion removed intravascular anti-FcRn F(ab′)$_2$ fragment. The silver grains were concentrated in the interstitium of the perimysium of the muscle bundles surrounding the vessels. There was no clustering of silver grains over the endothelial cells themselves (Fig. 3A), but in some cases silver grains could clearly be seen surrounding the capillaries. Signal was also detected

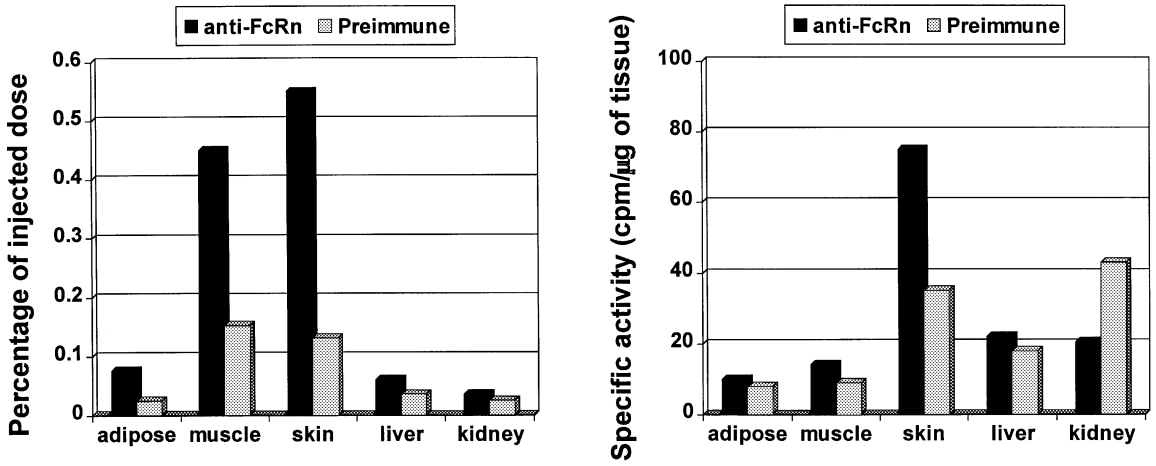

Fig. 2. Comparison of the uptake of anti-FcRn F(ab′)$_2$ and preimmune F(ab′)$_2$ fragments by skin, muscle, liver, adipose tissue and kidneys. (Left panel) Percentage of injected dose per organ. (Right panel) Radioactivity (in c.p.m.) per microgram of tissue per organ. Other organs analyzed (lungs, heart, spleen, small intestine and large intestine) have a percentage of injected dose <0.028% and are therefore not shown.

around vessels in endomysium. In sections from control animals there was no increase in silver grains adjacent to the vasculature (Fig. 3B). A similar distribution alongside the dermal vessels was identified in skin sections but the concentration of silver grains was lower (data not shown).

Tissue distribution of the Fc-hinge derivatives

The selective distribution of anti-FcRn F(ab′)$_2$ fragments in skin, muscle, fat and liver indicating that FcRn is expressed in these tissues was further analyzed by studying the distribution of a recombinant wild-type Fc-hinge fragment that binds to FcRn with high affinity. The localization of the wild-type Fc-hinge was compared with that of a mutant Fc-hinge fragment that does not bind at detectable levels to FcRn (6). As previously shown in BALB/c mice (21) the wild-type Fc-hinge has a β phase half-life of 82.9 ± 10.0 h while the mutant has a very short β phase half-life (15.6 ± 0.8 h) due to its inability to bind to FcRn (6,21). The distribution of the radiolabeled wild-type Fc-hinge and mutant in various tissues of mice at 3 days after injection is presented in Fig. 4. At this time the intravascular radioactivity was <10% of the injected dose. Consistent with the data obtained with F(ab′)$_2$ fragments, both skin and muscle were the major sites of wild-type Fc-hinge localization, whereas the mutant is concentrated primarily in kidney and, unexpectedly, in liver. The ratio between the distribution of wild-type and mutant is 25.9 for muscle, 21.7 for skin, 11.0 for adipose tissue and 0.3 for liver. The low wild-type/mutant ratio found in liver raises the question whether this organ is involved in the homeostasis of IgG or, similarly to the kidneys, whether it plays a role in excretion through its biliary function. The likelihood of this possibility was further strengthened by measuring the ratio between the radioactivity in the gall bladder and serum following injection of radiolabeled wild-type and mutant Fc-hinge fragments into mice. At 8 h following injection, the ratio was 4 times higher for mutant (0.68) than for wild-type (0.16), suggesting that the liver is not a barrier for the mutant which accumulates in the gall bladder and might subsequently be excreted through the intestine. The ratio between the percentage of injected dose localized in skin, muscle and adipose tissue for anti-FcRn F(ab′)$_2$ and preimmune F(ab′)$_2$ fragments is significantly lower than for wild-type and mutant Fc-hinge suggesting that only a fraction of the anti-FcRn F(ab′)$_2$ molecules binds to the FcRn present in these tissues.

The specific radioactivities (c.p.m./µg tissue) of muscle and skin are significantly higher for anti-FcRn F(ab′)$_2$ fragment and wild-type Fc-hinge respectively, showing that these two sites not only account for the largest fraction of the total injected dose but are also the most active organs involved in the specific uptake of anti-FcRn F(ab′)$_2$ fragment and wild-type Fc-hinge respectively.

Autoradiography of muscle at 8 h from mice injected with mutant Fc-hinge resulted in an absence of silver grains (Fig. 3C and D). In contrast, silver grains were evident in the sections of muscle from animals injected with wild-type Fc-hinge in a pattern similar to that in animals injected with anti-FcRn F(ab′)$_2$ fragment (Fig. 3E and F).

Tissue distribution of mouse IgG1 in β_2m-deficient mice

β_2m-deficient mice do not express functionally active FcRn (1–3,28) and therefore a comparison of the distribution of mouse IgG1 (mIgG1) in these mice (C57BL/6 background) and wild-type C57BL/6 mice might localize the site of functional FcRn expression and, by extension, of IgG homeostasis. The distribution of radiolabeled mIgG1 in the major tissues of these mice at 2 days post-injection is shown in Fig. 5. Consistent with the date obtained for both F(ab′)$_2$ and Fc-hinge fragments, mIgG1 is preferentially distributed in skin, muscle and adipose with $\beta_2m^{+/+}/\beta_2m^{-/-}$ ratios of 9.5, 2.9 and 5.0 for c.p.m./µg of tissue respectively.

Immunohistochemistry of FcRn

To determine if the autoradiographic patterns paralleled the distribution of FcRn, sections of muscle and liver were examined immunohistochemically using rabbit F(ab′)$_2$ anti-FcRn peptide antibody. The peptide used to make this antibody is

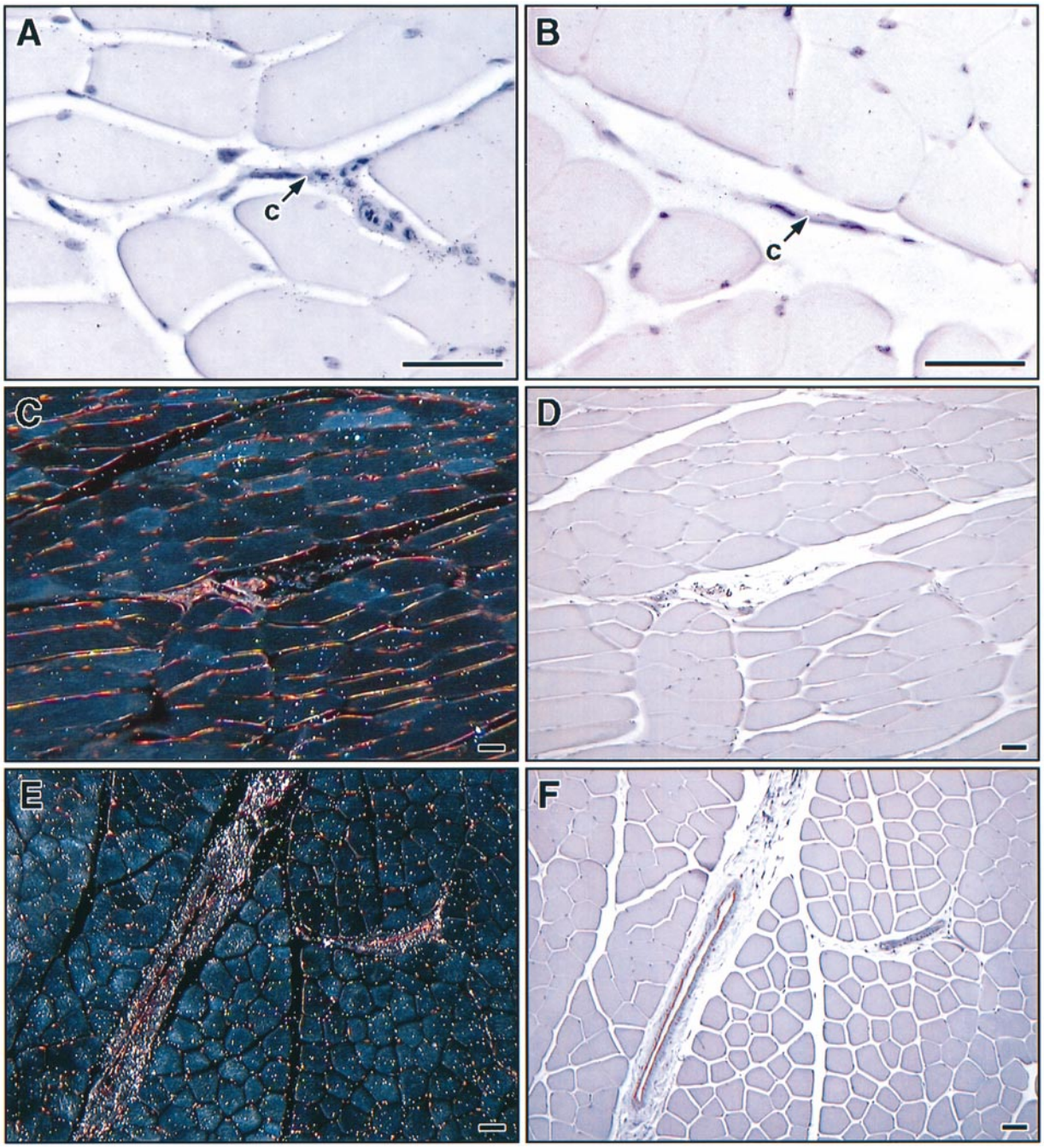

Fig. 3. Autoradiography of muscle of mice injected with [^{125}I]F(ab′)$_2$ anti-FcRn fragment and wild-type Fc-hinge. (A) Anti-FcRn F(ab′)$_2$ fragment, (B) Preimmune F(ab′)$_2$ fragments. (C) Mutant Fc-hinge. (E) Wild-type Fc-hinge. Plates (D) and (F) are contiguous to (C) and (E) respectively, and are stained for Von Willebrand's Factor VIII antigen to identify endothelial cells that line vessels. Note the silver grains associated with the vessels in plates (A) and (E). Plates (B) and (C) serve as controls and are negative. c, capillary; bar, 50 μm.

derived from the α2 domain of FcRn and this antibody was not used in the earlier studies as it was not available until recently. Following antigen retrieval of the formalin-fixed and paraffin-embedded tissues by heating in citrate buffer in a microwave, positive staining was detected in the endothelium of small arterioles and venules traversing the perimysium (Fig. 6A) and in scattered capillaries within the endomysium of the muscle. In sections of liver, strong positive staining was evident in the sinusoidal lining cells which consist of both endothelial cells and Kupffer cells. In addition, strong staining of the surface of the hepatocytes limited to that portion of the cell adjacent to the hepatic sinusoid was evident (Fig. 6B). The endothelium lining the central vein and portal vasculature was negative as were control sections. A similar but weaker staining was observed with absorbed anti-FcRn F(ab′)$_2$ fragment obtained by immunization of rabbits with recombinant

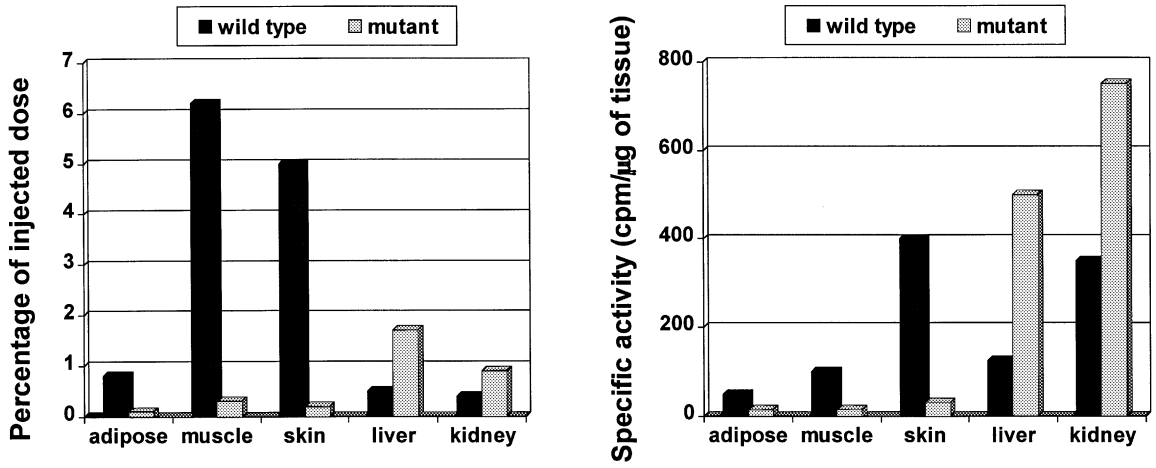

Fig. 4. Comparison of the uptake of wild-type and mutant Fc-hinge fragments in skin, muscle, liver, adipose tissue and kidneys. (Left panel) Percentage of injected dose per organ. (Right panel) Radioactivity (in c.p.m.) per microgram of tissue per organ. All other organs tested (see Fig. 3) have a percentage of injected dose <0.2%.

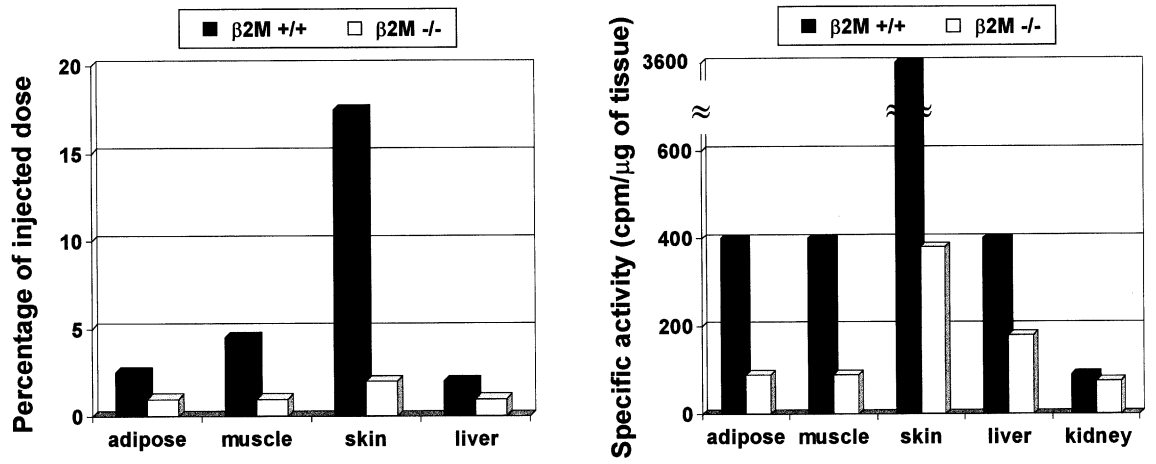

Fig. 5. Comparison of the uptake of mIgG1 by skin, muscle, liver, adipose tissue and kidneys in β_2m deficient (β2M–/–) and wild-type (β2M+/+) mice. (Left panel) Percentage of injected dose per organ. For both mouse strains, the percentage of injected dose for kidney was 0.1% or less and is therefore not shown. (Right panel) Radioactivity (in c.p.m.) per microgram of tissue per organ.

FcRn (data not shown). As a negative control, no staining was observed following treatment of tissues in the same way except without addition of the anti-FcRn antibody (not shown).

Detection of FcRn in cultured endothelial cells

Indirect immunofluorescence was used to detect FcRn in cultured mouse endothelial cells (SVEC) using anti-FcRn F(ab′)$_2$ fragments that had been preadsorbed on RMA cells to remove anti-β_2m and possible anti-MHC class I cross-reactivities. In permeabilized cells, a bright fluorescent staining was consistently present within the cytoplasm (but not on the membrane) surrounding the nuclei (Fig. 7A). The intracellular staining appeared as fluorescent dots which suggested that the labeling was associated with vesicular structures (Fig. 7B). Similar results were obtained using the anti-FcRn peptide antibody (not shown). In addition, incubation of permeabilized cells with wild-type Fc-hinge (that binds specifically to FcRn at pH 6.0) inhibited the interaction between the anti-FcRn antibody and the receptor, and, consequently, a very low level of fluorescence was detected (Fig. 7C). This indicates that the anti-FcRn F(ab′)$_2$ and Fc-hinge interact with overlapping sites of FcRn. No labeling was obtained in control experiments in which the anti-FcRn F(ab′)$_2$ fragment was omitted (Fig. 7D). The results indicate that FcRn is only localized intracellularly in SVEC cells and not on the cell membrane, and this is consistent with earlier data concerning FcRn localization on rat yolk sac cells by Roberts *et al.* (25). Furthermore, it indicates that following adsorption by RMA cells the anti-FcRn antibody does not cross-react with surface β_2m nor MHC class I molecules.

For the isolation of FcRn α chain and associated β_2m from SVEC cells, cells were biotinylated at room temperature for 30 min to label both surface bound and intracellular proteins (during which time the biotin penetrated the cells, analyzed

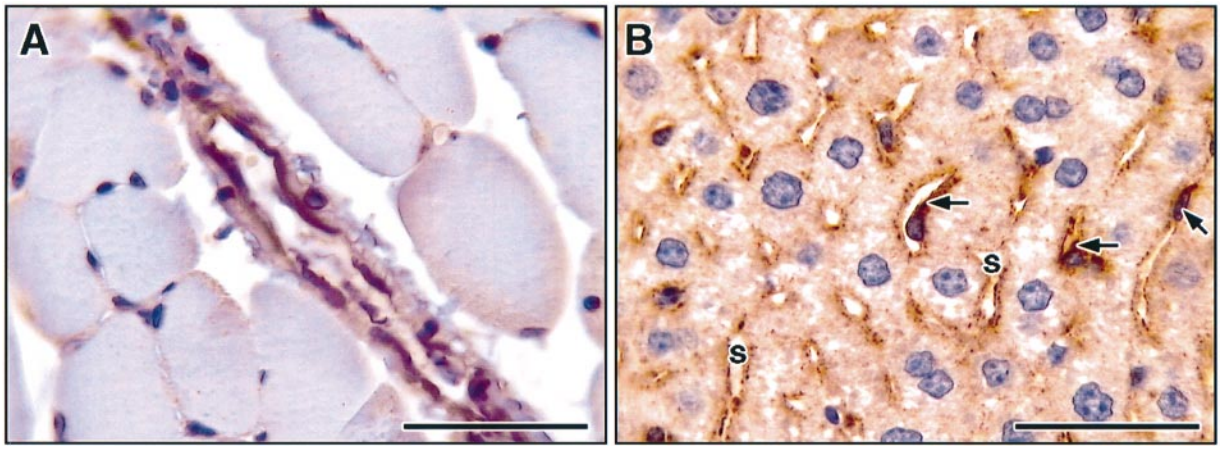

Fig. 6. Immunohistochemical detection of FcRn in muscle and liver of mice. (A) Muscle. (B) Liver. The endothelial cells lining the arteriole (A) are positive for FcRn, as are the sinusoidal lining cells and the surface of the hepatocytes adjacent to the sinusoids. Omission of anti-FcRn antibody resulted in no detectable staining. Arrow, sinusoidal lining cells; s, sinusoid; bar, 50 μm.

by immunblotting of cytosolic extracts of SVEC cells, using streptavidin–HRP; data not shown) and subsequently lysed. The lysate was run through an IgG1–Sepharose column and the pH 6.0 and 7.5 washes (the latter to elute bound FcRn which binds to IgG undetectably at this pH) (6) analyzed by immunoprecipitation with anti-FcRn polyclonal serum followed by Western blotting using streptavidin–HRP (Fig. 8). To demonstrate the specificity of the murine IgG1–Sepharose column, Western blots of samples (i.e. pH 6.0 and 7.5 washes) without immunoprecipitation are also shown using streptavidin–HRP for detection. The data clearly show that FcRn can be isolated in functionally active form from these cells. Although the polyclonal anti-mouse FcRn serum used for immunoprecipitation in this experiment was not absorbed on RMA cells, the identity of FcRn in the pH 7.5 washes is demonstrated by its characteristic, highly pH-dependent binding to IgG. Furthermore, FcRn α chain could be detected in both SVEC lysates and mIgG1–Sepharose eluates using the anti-FcRn peptide antibody in immunoblotting (data not shown).

Discussion

The data in this paper demonstrate that the receptor involved in regulating IgG catabolism, FcRn, is localized diffusely throughout the body. This is consistent with earlier data showing that FcRn α-chain mRNA is ubiquitously expressed in many murine cell types with the exception of cells of lymphocytic origin (1). The selective distribution of anti-FcRn $F(ab')_2$ antibody in skin and muscle is in agreement with previous data indicating that IgG catabolism is a diffuse process occurring primarily in skin, muscle and liver (13–15,29) in a compartment that is in rapid equilibrium with the intravascular compartment (16). This compartment might comprise the endothelial system of skin, muscle and adipose tissue microvessels and capillaries which are constantly exposed to circulating IgG. In rats, >90% of the extravascular IgG is located in the muscle, skin and adipose tissue (30,31), also indicating that these tissues might be directly involved in maintaining IgG homeostasis. Radiolabeled anti-FcRn $F(ab')_2$ was identified at the level of muscle and skin microvessels by autoradiography suggesting that this ligand was located alongside the microvessels but not in the lumen. We were not able to identify clusters of silver grains over endothelial cells and this may reflect the rapid transfer of the ligand from the intravascular to extravascular compartment rather than the absence of FcRn in endothelial cells. Consistent with this hypothesis, the presence of FcRn in endothelial cells in muscle was clearly demonstrated by staining the muscle sections with anti-FcRn $F(ab')_2$ fragments, which resulted in positive staining of endothelial cells in arterioles and some, but not all, capillaries. This heterogeneity in distribution of FcRn in the endothelium of various capillaries in muscle may be related to the well-known morphological differences between the endothelial cells lining various types of microcapillaries (32). The presence of FcRn on the endothelial cells of human muscle capillaries was also recently reported in a review paper (11).

The distribution of the wild-type Fc-hinge fragment which binds with high affinity to FcRn is similar to that observed for the anti-FcRn $F(ab')_2$ fragment. Relative to a mutant Fc-hinge fragment that does not bind detectably to FcRn, wild-type Fc-hinge preferentially localizes to muscle, skin and adipose tissue. In contrast to the anti-FcRn $F(ab')_2$, however, the ratio of wild-type/mutant in the liver is low. The higher levels of mutant Fc-hinge in the gall bladder relative to wild-type suggest that the mutant passes into this organ via the liver, which would also account for the higher relative levels of this protein in the liver. We have identified FcRn at the level of sinusoidal lining cells of liver as well as on the surface of hepatocytes adjacent to sinusoids suggesting that at this level FcRn may control not only the catabolism of IgG but also its transport from blood to bile. In this context, IgGs that bind to FcRn with higher affinity would be prevented from passing into bile, whereas the converse would be the case for IgGs that have poor binding affinity for FcRn. The positive staining of hepatocytes is in agreement with the biochemical data of Blumberg *et al.* (10) who detected FcRn by immunoprecipitation of rat liver extracts. The endothelial cell lining of

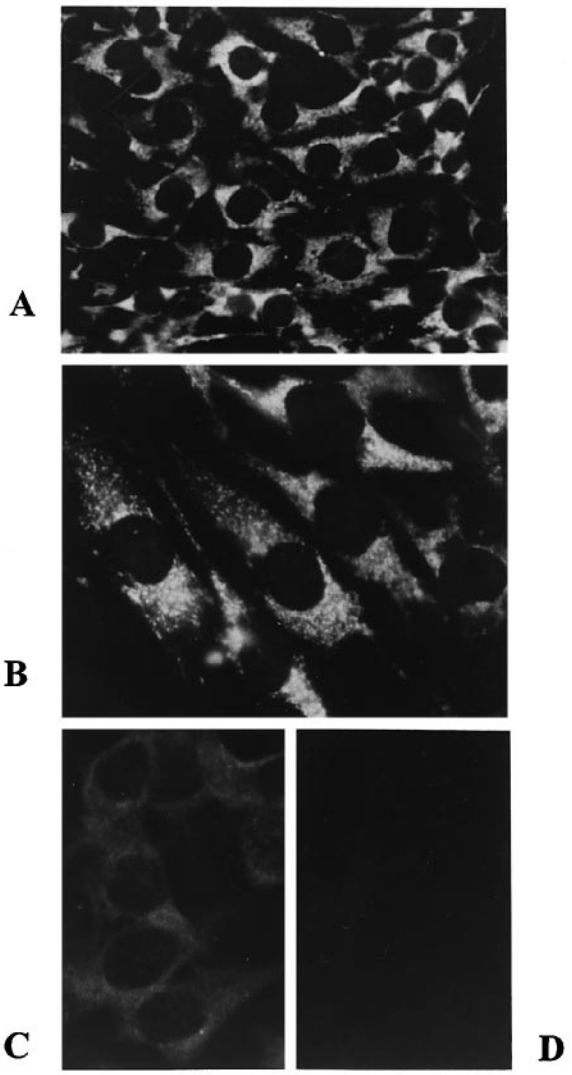

Fig. 7. Detection by indirect immunofluorescence of FcRn in SVEC cells with anti-FcRn F(ab′)$_2$ antibody followed by biotinylated secondary antibody and streptavidin–Texas Red. Cells grown on coverslips were fixed and permeabilized with cold methanol (A–D). As controls, the permeabilized cells were incubated with wild-type Fc-hinge at pH 6.3 before the immunostaining procedure (C) or the first antibody was omitted (D). Magnifications are: (A) ×280; (B)–(D) ×560.

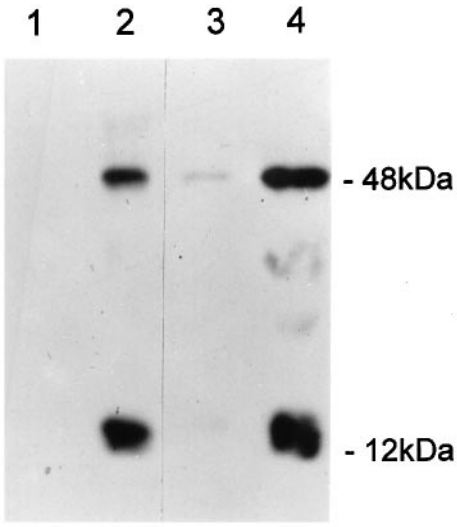

Fig. 8. Detection of FcRn in biotinylated cultured mouse endothelial cells (SVEC) using affinity chromatography (IgG–Sepharose) followed by Western blotting (12.5% SDS–PAGE) with streptavidin–HRP. Lane 1, pH 6.0 column wash; lane 2, pH 7.5 column wash; lane 3, pH 6.0 column wash followed by immunoprecipitation with anti-FcRn polyclonal serum; lane 4, pH 7.5 column wash followed by immunoprecipitation with anti-FcRn polyclonal serum.

central veins and portal vessels were negative, a finding that further underscores the heterogeneity of endothelial cells (32). The reasons for the differential distribution of wild-type Fc-hinge versus anti-FcRn F(ab′)$_2$ fragments in the liver are currently unclear and an area of further investigation.

The distribution of mIgG1 in β_2m-deficient and wild-type mice (both C57BL/6) confirms the observations with the anti-FcRn F(ab′)$_2$ and Fc-hinge fragments that FcRn–ligand interactions occur predominantly in skin, muscle and adipose tissue. mIgG1 accumulates in these tissues to much higher levels in wild-type mice than in β_2m-deficient mice that do not express functional FcRn (1–3,28). Taken together, the data show that if a ligand can interact with FcRn, it will be preferentially localized in these tissues indicating that these are the major sites at which IgG homeostasis occurs.

The presence of FcRn in mouse endothelial cells, indicated by immunohistochemistry of murine tissues, was further analyzed using cultured endothelial cells (SVEC cells). FcRn can be isolated from cell lysates using affinity chromatography on IgG–Sepharose, indicating that it is functionally active. The subcellular localization of FcRn in SVEC cells was investigated using anti-FcRn F(ab′)$_2$ fragment and indirect immunofluorescence. FcRn is not present on the membrane of SVEC cells but can be detected in the cytoplasm surrounding the nuclei. The appearance of the staining suggests that the labeling may be associated with vesicular structures. This finding is reminiscent of the electron microscopic data of Roberts *et al.* (25) indicating the presence of FcRn in the cytoplasm but not on the membrane of rat fetal yolk sac. Our results are also consistent with the possible involvement of the endothelial cells in the catabolism of IgG by a mechanism that does not require the presence of FcRn on the cell surface (27). The transfer of IgG from the intravascular to interstitial compartment may involve FcRn-mediated transcytosis or alternatively, may occur through intercellular junctions of endothelial cells without the involvement of FcRn. It is also possible that both pathways of transport are involved in mediating the capillary permeability of IgG, in an analogous way to that shown for the transport of albumin through endothelial cells (33). The exchange of plasma proteins through endothelial cells is bidirectional (34) involving both the luminal and the abluminal faces of the cells. Therefore, the regulation of IgG levels by endothelial cells may result from the salvaging and exocytosis of the molecules that penetrate the cells from both intra- and extravascular compartments. IgG not bound to FcRn may be destined for destruction and this would explain how IgG homeostasis is maintained.

In summary, our data support the involvement of FcRn in endothelial cells in regulating the levels of serum IgG. This is consistent with the close contact of these cells with the vasculature. The molecular mechanism by which FcRn carries out this function remains an area for future study.

Acknowledgements

We thank May Fang Tsen for skillful assistance with pharmacokinetic experiments, Robert Webb for assistance with histological studies, John Shelton for technical support, and Luminita Radulescu and Olga Starodub for invaluable help with immunofluorescence staining. This work was supported by grants from the NIH (AI39167), the Texas Coordinating Board (003660-006) and Robert Welch Foundation (I-1333).

Abbreviations

β_2m	β_2-microglobulin
FcRn	neonatal Fc receptor
HRP	horseradish peroxidase
SVEC	SV40-transformed mouse endothelial cells

References

1 Ghetie, V., Hubbard, J. G., Kim, J.-K., Tsen, M. F., Lee, Y. and Ward, E. S. 1996. Abnormally short serum half-lives of IgG in beta 2-microglobulin-deficient mice. *Eur. J Immunol.* 26:690.
2 Junghans, R. P. and Anderson, C. L. 1996. The protection receptor for IgG catabolism is the beta 2-microglobulin-containing neonatal intestinal transport receptor. *Proc. Natl Acad. Sci. USA* 93:5512.
3 Israel, E. J., Wilsker, D. F., Hayes, K. C., Schoenfeld, D. and Simister, N. E. 1996. Increased clearance of IgG in mice that lack beta 2-microglobulin: possible protective role of FcRn. *Immunology* 89:573.
4 Simister, N. E. and Mostov, K. E. 1989. An Fc receptor structurally related to MHC class I antigens. *Nature* 337:184.
5 Medesan, C., Matesoi, D., Radu, C., Ghetie, V. and Ward, E. S. 1997. Delineation of the amino acid residues involved in transcytosis and catabolism of mouse IgG1. *J. Immunol.* 158:2211.
6 Popov, S., Hubbard, J. G., Kim, J.-K., Ober, B., Ghetie, V. and Ward, E. S. 1996. The stoichiometry and affinity of the interaction of murine Fc fragments with the MHC class I-related receptor, FcRn. *Mol. Immunol.* 33:521.
7 Ghetie, V., Popov, S., Borvak, J., Radu, C., Matesoi, D., Medesan, C., Ober, R. J. and Ward, E. S. 1997. Increasing the serum persistence of an IgG fragment by random mutagenesis. *Nature Biotechnol.* 15:637.
8 Simister, N. E. and Mostov, K. E. 1989. Cloning and expression of the neonatal rat intestinal Fc receptor, a major histocompatibility complex class I antigen homolog. *Cold Spring Harbor Symp. Quant. Biol.* 54:571.
9 Story, C. M., Mikulska, J. E. and Simister, N. E. 1994. A major histocompatibility complex class I-like Fc receptor cloned from human placenta: possible role in transfer of immunoglobulin G from mother to fetus. *J. Exp. Med.* 180:2377.
10 Blumberg, R. S., Koss, T., Story, C. M., Barisani, D., Polischuk, J., Lipin, A., Pablo, L., Green, R. and Simister, N. E. 1995. A major histocompatibility complex class I-related Fc receptor for IgG on rat hepatocytes. *J. Clin. Invest.* 95:2397.
11 Junghans, R. P. 1997. Finally! The Brambell receptor (FcRB). Mediator of transmission of immunity and protection from catabolism for IgG. *Immunol. Res.* 16:29.
12 Brambell, F. W. R. 1970. *The Transmission of Passive Immunity from Mother to Young*, p. 42. North-Holland, Amsterdam.
13 Henderson, L. A., Baynes, J. W. and Thorpe, S. R. 1982. Identification of the sites of IgG catabolism in the rat. *Arch. Biochem. Biophys.* 215:1.
14 Moldoveanu, Z., Epps, J. M., Thorpe, S. R. and Mestecky, J. 1988. The sites of catabolism of murine monomeric IgA. *J. Immunol.* 141:208.
15 Moldoveanu, Z., Moro, J., Radl, J., Thorpe, S. R., Komiyama, K. and Mestecky, J. 1990. Site of catabolism of autologous and heterologous IgA in non-human primates. *Scand. J. Immunol.* 32:577.
16 Waldmann, T. A. and Strober, W. 1969. Metabolism of immunoglobulins. *Progr. Allergy* 13: 1.
17 Mariani, G. and Strober, W. 1991. Immunoglobulin metabolism. In Metzger, H., ed., *Fc Receptors and the Action of Antibodies*, p. 94. American Society for Microbiology, Washington, DC.
18 O'Connell, K. A. and Edidin, M. 1990. A mouse lymphoid endothelial cell line immortalized by simian virus 40 binds lymphocytes and retains functional characteristics of normal endothelial cells. *J. Immunol.* 144:521.
19 Chien, Y. H., Gascoigne, N. R. J., Kavaler, J., Lee, N. E. and Davis, M. M. 1984. Somatic recombination in a murine T-cell receptor gene. *Nature* 309:322.
20 Lunggren, H. G. and Karre, K. 1985. Host resistance directed selectively against H-2-deficient lymphoma variants. Analysis of the mechanism. *J. Exp. Med.* 162:1745.
21 Kim, J. K., Tsen, M. F., Ghetie, V. and Ward, E. S. 1994. Identifying amino acid residues that influence plasma clearance of murine IgG1 fragments by site-directed mutagenesis. *Eur. J. Immunol.* 24:542.
22 Simister, N. E., Story, C. M., Chen, H. L. and Hunt, J. S. 1996. An IgG-transporting Fc receptor expressed in the syncytiotrophoblast of human placenta. *Eur. J. Immunol.* 26:1527.
23 Caster, W. O., Poncelet, J., Simon, A. B. and Armstrong, W. D. 1956. Tissue weights of the rat. 1. Normal values determined by dissection and chemical methods. *Proc. Soc. Exp. Biol. Med.* 91:122.
24 Strobel, J. L., Cady, S. G., Borg, T. K., Terracio, L., Baynes, J. W. and Thorpe, S. R. 1986. Identification of fibroblasts as a major site of albumin catabolism in peripheral tissues. *J. Biol. Chem.* 261:7989.
25 Roberts, D. M., Gunthert, M. and Rodewald, R. 1990. Isolation and characterization of the Fc receptor from the fetal yolk sac of rat. *J. Cell Biol.* 111: 867.
26 Towbin, H., Staehelin, T. and Gordon, J. 1979. Electrophoretic transfer of proteins from polyacrylamide gels to nitrocellulose sheets: procedure and some applications. *Proc. Natl Acad. Sci. USA* 76:4350.
27 Ghetie, V. and Ward, E. S. 1997. FcRn: the MHC class I-related receptor that is more than an IgG transporter. *Immunol. Today* 18:592.
28 Zijlstra, M., Bix, M., Simister, N. E., Loring, J. M., Raulet, D. H. and Jaenisch, R. 1990. β_2-microglobulin deficient mice lack $CD4^-8^+$ cytolytic T cells. *Nature* 344:642.
29 Jones, E. A. and Waldmann, T. A. 1972. The mechanism of intestinal uptake and transcellular transport of IgG in the neonatal rat. *J. Clin. Invest.* 51:2916.
30 Dewey, W. C. 1959. Vascular–extravascular exchange of ^{131}I plasma proteins in the rat. *Am. J. Physiol.* 197:423.
31 O'Connor, S. W. and Bale, W. F. 1984. Accessibility of circulating immunoglobulin G to the extravascular compartment of solid rat tumors. *Cancer Res.* 44:3719.
32 Simionescu, M. and Simionescu, N. 1986. Functions of the endothelial cell surface. *Annu. Rev. Physiol.* 48:279.
33 Schnitzer, J. E. and Oh, P. 1994. Albondin-mediated capillary permeability to albumin. Differential role of receptors in endothelial transcytosis and endocytosis of native and modified albumins. *J. Biol. Chem.* 269:6072.
34 Simionescu, N., Simionescu, M. and Palade, G. E. 1976. Structural-functional correlates in the transendothelial exchange of water-soluble macromolecules. *Thromb. Res.* 8:257.